JOURNAL OF Materials CHEMISTRY

Alkylammonium derivatives of layered alkali silicates and micro- and mesoporous materials: I. Lithium sodium silicate (silinaite)

Peter Thiesen,[a] Klaus Beneke[b] and Gerhard Lagaly*[b]

[a]*Department of Mechanical Engineering, Institute for Thermodynamics, University of the Federal Armed Forces, D-22039 Hamburg, Germany*
[b]*Institute of Inorganic Chemistry, University of Kiel, D-24098 Kiel, Germany. E-mail: h.mittag@email.uni-kiel.de*

Received 20th December 1999, Accepted 8th February 2000
Published on the Web 31st March 2000

The layered lithium sodium silicate silinaite exchanges alkylammonium ions for interlayer lithium and sodium ions. This exchange increases the disorder of the structure and leads to transformation of many Q^3 silicon oxygen groups into Q^4 groups. Owing to their large size the alkylammonium ions displace only a part of the inorganic interlayer cations. The remaining lithium and sodium ions are replaced by protons, and the silanol groups (Q^3 Si) can condense to siloxane groups (Q^4 Si). Calcination of the alkylammonium derivatives at 350–550 °C yields mesoporous materials with mesopore volumes of between 130 and 390 μL g^{-1} and micropore volumes of between 25 and 110 μL g^{-1}. The diameters of the mesopores lie between 1.7 and 2.9 nm (from mesopore volumes and surface areas). In the same way, porous materials with similar properties were prepared from other silica sources like sodium metasilicalite, δ-$Na_2Si_2O_5$ (SKS-6), and even water glass solutions. A mechanism is proposed based on the aggregation of alkylammonium ions carrying caps of the fragmented layers.

Introduction

Layered compounds are becoming of increasing interest as active inorganic fillers in polymer nanocomposites. Clay minerals are often used[1] but encouraging results have also been obtained with alkali silicates and crystalline silicic acids.[1–3] Compatibility with the polymer often requires hydrophobization of the inorganic material. Cation exchange with alkylammonium ions is an important reaction to make the mineral hydrophobic. Another field of potential applications has been developed by the transformation of layered alkali silicates into porous materials.[4–12]

Different applications require different types of layered alkali silicates. Zweier single-layer phyllosilicates (classification of Liebau[13,14]) like $Na_2Si_2O_5$,[15–17] kanemite $NaHSi_2O_5 \cdot 3H_2O$,[18–28] $KHSi_2O_5 \cdot 2H_2O$,[29–31] silinaite $NaLiSi_2O_5 \cdot 2H_2O$,[32–34] makatite $Na_2Si_4O_8(OH)_2 \cdot 4H_2O$,[19,20,24,35–37] and octosilicate $Na_2Si_8O_{17} \cdot 10H_2O$[20,21,38–40] consist of folded sheets of silicon–oxygen tetrahedra. The sheets are highly flexible, and the silicates are less suitable as inorganic fillers. Silicates with condensed tetrahedral sheets like magadiite[19–21,24,38,39,41–47] and kenyaite[19,20,24,38,39,42,47,48] are more effective fillers for polymers. On the other hand, the flexibility of single layer silicates enables the preparation of mesoporous silica. Kanemite was dispersed in an alkaline aqueous solution of hexadecyltrimethylammonium chloride. After lowering the pH to 8.5 the product was filtered, washed with water, and calcined at 700 °C or 1000 °C.[4–12] It was assumed that the flexible silicate layers wind around the aggregated surfactants. Condensation of the silanol groups during calcination resulted in an almost hexagonal honeycomb pattern of hollow silica tubes. This material was called a folded sheets mesoporous material, FSM. This reaction is not restricted to kanemite as starting material, but can also be performed with other single-layer silicates and even water glass solutions as reported in this paper.

Experimental

Silicates

Silinaite, $NaLiSi_2O_5 \cdot 2H_2O$, was prepared by heating a dispersion of silica (Kieselgel, Merck, Germany) in an aqueous solution of lithium hydroxide and sodium hydroxide at 125 °C for 4 days. Molar ratios used: $LiOH/SiO_2 = 0.5$; $NaOH/SiO_2 = 0.5$; $H_2O/SiO_2 = 10$.[34] We used thick-walled Teflon flasks with nearly gas-tight screw-on-type caps. The precipitate was washed with small amounts of water and air-dried. The product corresponded to sample 89X described before.[34]

Kanemite, $NaHSi_2O_5 \cdot 3H_2O$, was prepared from a NaOH–SiO_2 mixture (molar ratio 1 : 1). NaOH was dissolved in a small amount of water. This solution was diluted with ethanol (or methanol) so that the required amount of silica could easily be dispersed forming a homogeneous slurry which was dried at 100 °C, then heated to 700 °C for 5.5 h. Rehydration in water yielded kanemite.[18] δ-$Na_2Si_2O_5$ (SKS-6) was obtained from Hoechst Comp. (Germany) and sodium metasilicate (Na_2SiO_3) from Condea Chemie (Germany). These silicates are produced as detergent additives (builder).[15] Water glass was from Merck (Germany).

Alkylammonium derivates

The alkylammonium derivatives were prepared by dispersing 1.5 g of silinaite in 50 mL of an aqueous solution of alkylammonium chloride at 65 °C for 48 h. The alkylammonium chloride solutions were obtained by adding 2 M hydrochloric acid to an aqueous solutions of the alkylamine $C_nH_{2n+1}NH_2$ ($n = 1, 2, ..., 10$) until pH = 7 was reached.

Silinaite was also reacted with several quaternary alkylammonium halogenides: dodecyltrimethylammonium bromide (DDTMA), tetradecyltrimethylammonium bromide (TDTMA), hexadecyltrimethylammonium bromide (HDTMA), and *N*-cetylpyridinium chloride (CP). In addition,

a mixture of tetraethylammonium bromide (TEA) and HDTMA was used. To prepare 0.1 M aqueous solutions of the surfactants the required amounts (3.08 g DDTMA, 3.36 g TDTMA, 3.64 g HDTMA, 3.39 g CP, and 3.5 g TEA + 3.64 g HDTMA) were dispersed in 100 mL water and heated to 65 °C until the surfactant was dissolved. 5 g silinaite were dispersed (Ultra Turrax) in 50 mL water before 100 mL of the surfactant solution were added. Following the procedure described by Kuroda *et al.*,[5,7] the pH was adjusted to 12.5, and the dispersion was held at 70 °C for 3 h. After cooling to room temperature, 2 M hydrochloric acid was added dropwise to decrease the pH to 8.5. The dispersion was heated again to 70 °C for 3 h, then filtered. The product was washed with 100 mL water and dried at 65 °C. Amounts of 1 g of these samples were calcined at 350 °C, 450 °C, 550 °C, and 700 °C for 6 h.

In the same way, kanemite, δ-$Na_2Si_2O_5$, and sodium metasilicate were reacted with the quaternary alkylammonium salts and calcined at 550 °C. Also, 20 mL water glass were reacted with the same amounts of surfactants.

The ^{29}Si-MAS-NMR spectra were obtained with a Bruker AM 400 instrument at 293 K (spinning rate 5 kHz, frequency 79.496 MHz; aquisition time 17 ms, pulse repetition time 60 s, high power decoupling). Accumulations amounted to 700 scans. Chemical shifts are reported relative to gaseous tetramethylsilane.

Gas adsorption measurements

The nitrogen adsorption at 77 K was measured in a home-made volumetric instrument.[49,50] The relative pressure p/p_0 was increased in steps of 0.04 from 0 to 0.965 (adsorption branch), then decreased to 0.005 (desorption branch). Equilibration was achieved within 1 min. The apparent specific surface area was calculated by the BET equation (surface area of the nitrogen molecule:[51–53] 0.162 nm^2). The calculated specific surface area does not correspond to the real surface area when micropores (pores with diameters <2 nm) are present. The presence of micropores was tested with *t*-plots.[50–52] In these diagrams the amount of nitrogen adsorbed at every relative pressure is plotted against the statistical thickness t of the adsorbed layer at the same pressure. The values of t are obtained from standard curves.

In the ideal case the *t*-curve is linear; the specific surface area and the micropore volume are obtained from the intercept and the slope, respectively. A problem consists of the correct choice of the standard isotherm. As discussed below, we used theoretical standard isotherms[54] calculated for BET *C*-values of 20–30.

The amounts of nitrogen adsorbed are given in volumes of gaseous nitrogen (in cm^3 g^{-1} at STP). The micropore volume is expressed by the volume of liquid nitrogen (in μL g^{-1}). With a molar volume of gaseous nitrogen at STP (22414 cm^3) and of liquid nitrogen at 77 K (34.67 cm^3) one obtains

$$V(\mu\text{L g}^{-1}) = \frac{34.67}{22414} \times 10^3\ V(\text{cm}^3\ \text{g}^{-1}) = 1.5468\ V(\text{cm}^3\ \text{g}^{-1}) \quad (1)$$

The lower density of the nitrogen molecules in ultramicropores (diameter <0.7 nm) in comparison with the bulk was considered by the factor 1.091.[50,53]

Results

Alkylammonium silinaites

Silinaite consists of silicate layers of unbranched zweier single chains. The layers are connected by [LiO_4] tetrahedra and [$Na(H_2O)_4O_2$] octahedra[33] (Fig. 1). When the lithium and sodium interlayer cations are replaced by alkylammonium ions, the structure must be distorted. The broad reflections in the X-ray diagrams (Fig. 2) indicate a high degree of disorder. The peak at $2\theta \approx 9°$ probably indicates the stacking distance of the disordered layers and reveals an average basal spacing of 1 nm. Surprisingly, the powder diagrams of silinaite with longer alkylammonium ions showed an additional sharp low-angle reflection ($2\theta = 3.51°$, $d = 25$ nm for heptylammonium ions; $2\theta = 2.77°$, $d = 32$ nm for decylammonium ions).

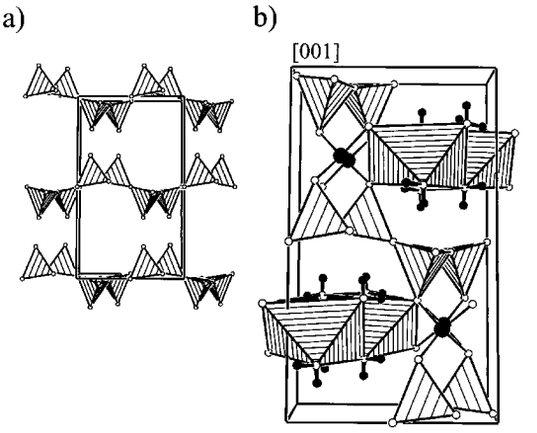

Fig. 1 The layer structure of silinaite:[33] a) the silicate layers, b) the [LiO_4] tetrahedra and [$Na(H_2O)_4O_2$] octahedra between the layers (○ oxygen, • protons of H_2O, ● lithium ions).

Structural changes during the alkylammonium exchange were also evident from the IR spectra. The alkylammonium derivatives showed similar spectra which differed strongly from the spectrum of the original silinaite (Fig. 3). The group of absorption bands between 1200 cm^{-1} and 960 cm^{-1} in silinaite were assigned as asymmetric stretching vibrations of Si–O–Si groups and stretching vibrations of Si–O$^-$.[27,55,56] The symmetric Si–O–Si stretching vibrations yielded bands between 800 and 600 cm^{-1}. Bending vibrations and M–O stretching modes were indicated below 500 cm^{-1}; for details see ref. 56. After alkylammonium exchange the bands were broadened and were not resolved. Also, the stretching vibrations of OH and H_2O at 3200–3550 cm^{-1} (ref. 56) were no longer resolved. The three signals at 2964, 2924, and 2859 cm^{-1} were attributed to stretching vibrations of the methyl and methylene groups of the alkyl chains.

The ^{29}Si-MAS-NMR spectra (Fig. 4) also revealed the structural changes. Silinaite showed a strong signal at

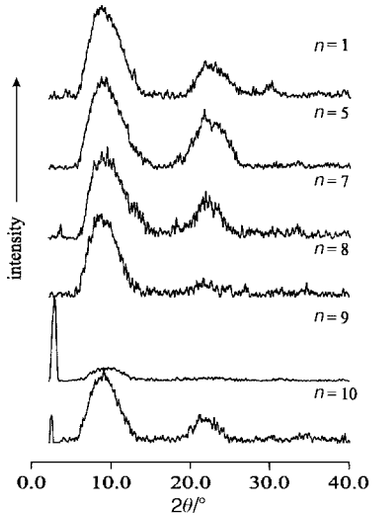

Fig. 2 X-Ray diffractograms (Cu-Kα) of alkylammonium silinaites after drying at 65 °C. n = number of carbon atoms in the alkylammonium ion.

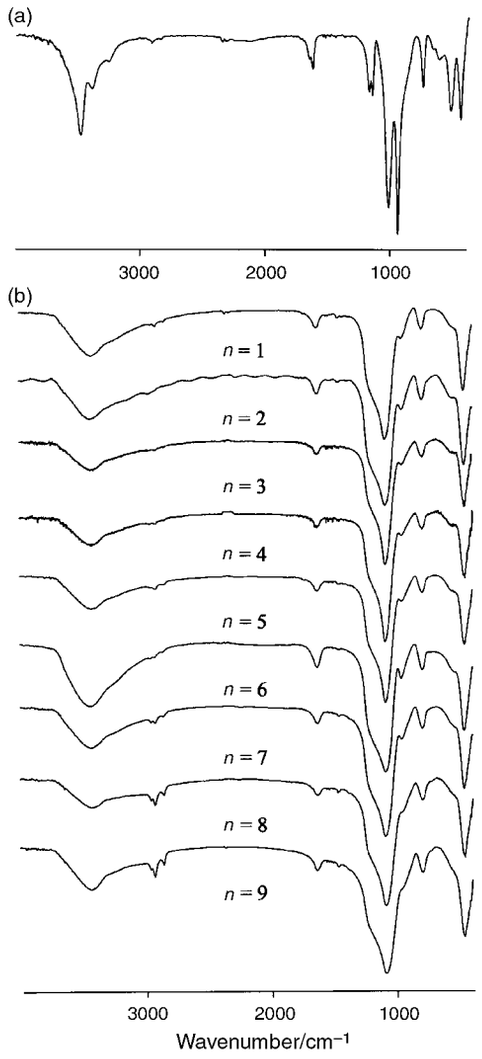

Fig. 3 IR spectra of silinaite (a) and the alkylammonium derivatives with *n* carbon atoms in the alkyl chain (b).

δ −92.46 (with rotational side bands at δ −29.33 and −155.43)[34] which indicates the presence of Q^3 groups as expected from the crystal structure. Signals of Q^4 and Q^2 groups were absent. The corresponding crystalline acid (obtained by exchanging the sodium and lithium ions by protons[34]) revealed two broad peaks at δ −101.8 and −111.6 corresponding to Q^3 and Q^4 groups. The alkylammonium derivatives also showed Q^3 peaks and two broad peaks at δ *ca.* −110 (Q^4 groups) (Fig. 4, Table 1). The chemical shift related to the Q^3 groups decreased with increasing alkyl chain length from δ −99.79 (methylammonium ions) to −100.50 (hexylammonium ions) and then increased to δ −98.6 for the longest chains. The chemical shift for the Q^4 groups also decreased from the methylammonium to the hexylammonium derivative but changed in an unregular manner for longer alkyl chains. The peak area of the Q^3 groups occupied 20–32% of the total area of the Q^3+Q^4 groups (calculated by deconvolution in terms of overlapping Gaussian peaks). The nonylammonium derivative showed an exceptionally high Q^3 peak. Because of very long relaxation times for silicates (of the order of hours; D. Heidemann (Berlin), personal communication, see also ref. 47) the molar ratio of Q^3 and Q^4 groups cannot be simply obtained from the peak intensity or areas.

Surfactant-templated porous materials from silinaite

Silinaite was reacted with several quaternary alkylammonium halogenides. The X-ray diagrams of the dried derivatives

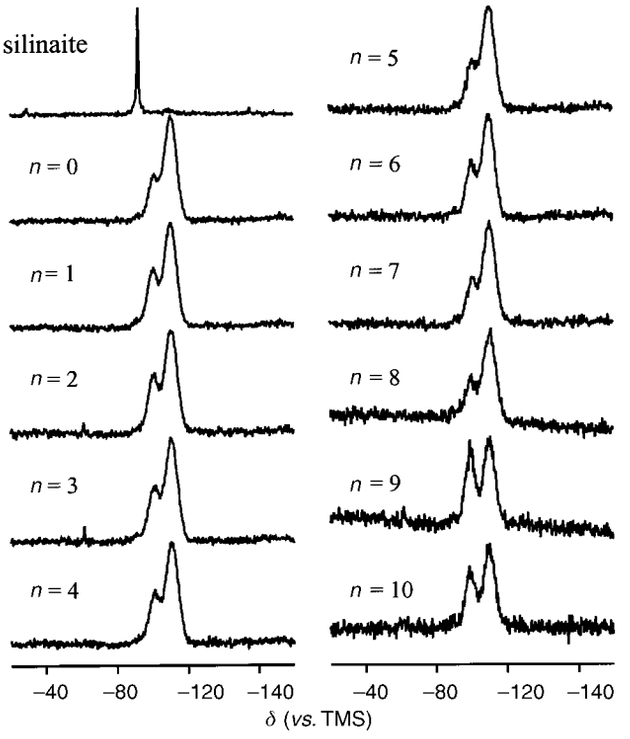

Fig. 4 ^{29}Si-MAS-NMR spectra of silinaite, sample 89X, and the alkylammonium derivatives with *n* carbon atoms in the alkyl chain (*n* = 0: ammonium derivative).

Table 1 Chemical shifts in the ^{29}Si-MAS-NMR spectra of silinaite and the alkylammonium derivatives with *n* carbon atoms in the alkyl chain (*n* = 0: ammonium derivative), deconvolution in terms of overlapping Gaussian peaks

n	δ	δ
NaLi	−92.47	—
0	−100.50	−110.32
1	−99.79	−109.98
2	−100.01	−110.15
3	−100.04	−110.22
4	−100.16	−110.32
5	−100.59	−110.61
6	−100.50	−110.63
7	−100.20	−110.23
8	−98.61	−110.95
9	−99.33	−110.13
10	−98.45	−111.17

showed broad peaks (Fig. 5) like the derivatives with primary alkylammonium ions, and an intense sharp reflection between $2\theta = 2^\circ$ and $2\theta = 3^\circ$ (Fig. 2; please note the different scale of the 2θ axis!).

The ^{29}Si-MAS-NMR spectra showed two broad peaks (Fig. 6) which again indicated the presence of Q^3 and Q^4 groups. Heating to 550 °C greatly increased the proportion of Q^4 groups (the presence of Q^3 was only indicated by a shoulder on the Q^4 peak). Thus, a considerable portion of the silanol groups (Q^3) were condensed to siloxane groups. At 700 °C the samples transformed into quartz which was indicated by a sharp peak at δ −107.1.

The adsorption isotherms of silinaite, its TDTMA derivative, and this derivative heated to 550 °C (Fig. 7) illustrate the enormous increase of nitrogen adsorption after calcination. The adsorption isotherm of the calcined organic derivative showed a very small hysteresis loop at $p/p_0 > 0.4$. The *t*-plots of silinaite and the TDTMA derivative were linear and passed through the origin (Fig. 8); micropores were absent. In contrast, the *t*-curve of the calcined organic derivative revealed

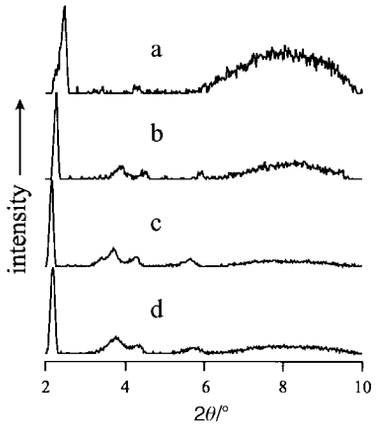

Fig. 5 X-Ray diffractograms (Cu-Kα) of alkylammonium silicates dried at 65 °C: a) TDTMA derivative of silinaite, b) HDTMA derivative of silinaite, c) HDTMA and metasilicate, d) HDTMA and water glass solution.

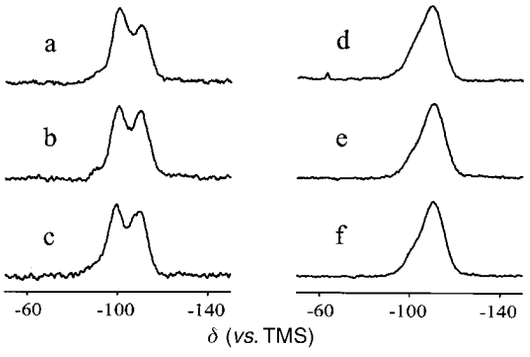

Fig. 6 ^{29}Si-MAS-NMR spectra of the TDTMA derivative of a,d) silinaite, b,e) metasilicate, c,f) water glass solution; a–c) air-dried, d–f) calcined at 550 °C.

two linear sections. The micropore volume and the surface area were calculated from the linear section at smaller *t*-values (Table 2).

The amount of nitrogen adsorbed by TDTMA–silinaite reached a maximum after calcination at 450 °C (Fig. 9, Table 2). Formation of quartz at 700 °C reduced the specific surface area to 5 $m^2 g^{-1}$. The micropore volume was highest after calcination at 350 °C.

The nitrogen adsorption isotherms for the other alkylammonium derivatives (DDTMA, HDTMA, CP, HDTMA+ TEA) showed the same behavior. The typical shape of type IV isotherms was more pronounced for the longer surfactants. The *t*-curves were similar to those shown in Fig. 8. The specific surface area and the micropore volume increased with the alkyl chain length of the alkyltrimethylammonium derivatives (Tables 2, 3). The values of the calcined cetylpyridinium silinaite were distinctly smaller, even below those of the DDTMA derivative (Table 2). The effect of tetraethylammonium ions to restrict the interlayer expansion[58] is also evident. The presence of these ions reduced the specific surface area and the pore volume of the HDTMA derivative (Table 2).

Porous materials from other silicate sources

Porous materials very similar to those described above were obtained from δ-$Na_2Si_2O_5$ (SKS-6), Na_2SiO_3 (metasilicate) and even water glass solutions.

The X-ray diagrams corresponded to those of the silinaite derivatives (Fig. 5) and showed the intense sharp reflection at $2\theta = 2$–$3°$. The *d*-value of this reflection was 3.89 nm (HDTMA silinaite), 4.04 nm (HDTMA metasilicate), and 4.10 nm (HDTMA derivative of water glass). The ^{29}Si-MAS-NMR

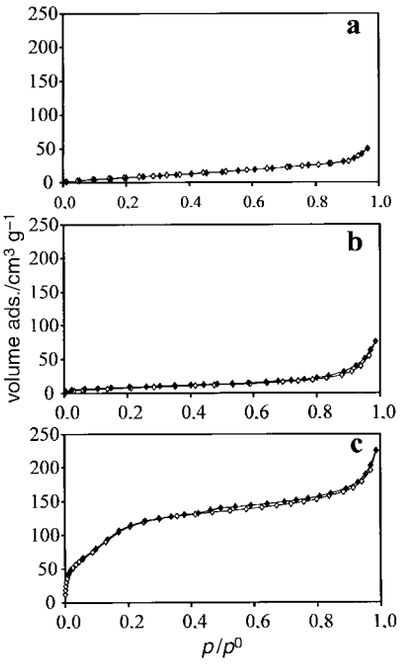

Fig. 7 N_2 adsorption isotherms (◇ adsorption, ◆ desorption, cm^3 N_2 (STP) g^{-1}, 77 K): a) silinaite, b) TDTMA derivative dried at 65 °C, c) TDTMA derivative calcined at 550 °C.

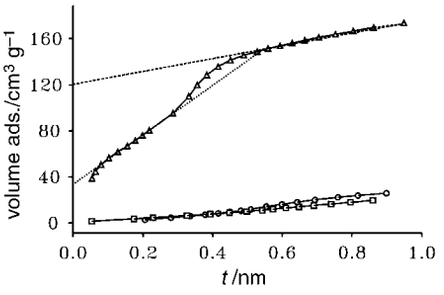

Fig. 8 *t*-Plots of silinaite (□), TDTMA silinaite dried at 65 °C (○), TDTMA silinaite calcined at 550 °C (△).

spectra also consisted of the broad peaks attributed to Q^3 and Q^4 groups. After calcination at 550 °C one peak with a shoulder corresponding to Q^3 groups indicated the increased proportion of Q^4 groups.

Also, the nitrogen adsorption isotherms and the *t*-curves were of the same type, and large amounts of nitrogen were adsorbed (Fig. 10). Only the isotherm of the $Na_2Si_2O_5$ derivative was of different shape and opened to a hysteresis loop at a relative pressure of 0.8 (Fig. 11). The *t*-curve of the calcined SKS-6 derivative showed linear sections at low and high *t*-values like the other samples. Because of the presence of micropores, the specific BET surface area calculated from the adsorption isotherm (Table 2) exceeded 800 $m^2 g^{-1}$ for calcined HDTMA silinaite and metasilicate; the water glass derivative yielded a value of 688 $m^2 g^{-1}$ and the SKS-6 463 $m^2 g^{-1}$. However, these are apparent values. The surface areas derived from the *t*-plots (adsorption branches) were 521–529 $m^2 g^{-1}$ (for silinaite, metasilicate, water glass) and 346 $m^2 g^{-1}$ (for SKS-6). The micropore volume varied between 55 and 113 μL g^{-1} (Table 4).

Discussion

Alkylammonium exchange

The structure of the silicate sheet (Fig. 1), in particular the degree of folding, will not remain unchanged when the sodium

Table 2 Specific surface area and micropore volume of trimethylalkylammonium silinaites calcined at 350–700 °C (from the adsorption branch of the isotherms)

Sample	Specific surface area/$m^2\ g^{-1}$		Micropore volume/$\mu L\ g^{-1}$[b]
	Apparent[a]	From *t*-plot[b]	
NH_4^+	30		6.6
DDTMA, 550 °C	317	274	25.7
TDTMA, 65 °C	28	27	1
TDTMA, 350 °C	526	331	75.2
TDTMA, 450 °C	610	443	59.6
TDTMA, 550 °C	461	338	50.2
TDTMA, 700 °C	7	5	1
HDTMA, 550 °C	817	529	109.7
CP, 550 °C	267	181	38.0
HDTMA + TEA, 550 °C	247	0197	30.9

[a]From the BET equation. [b]From the linear *t*-plot at low p/p_0.

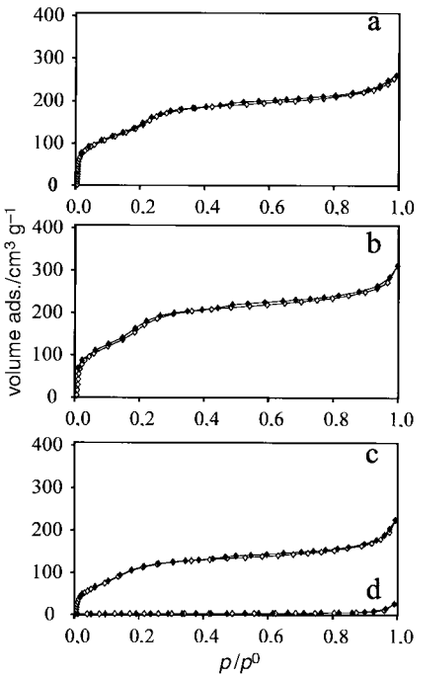

Fig. 9 N_2 adsorption isotherms (◇ adsorption, ◆ desorption, cm^3 N_2 (STP) g^{-1}, 77 K). TDTMA silinaite calcined at a) 350 °C, b) 450 °C, c) 550 °C, d) 700 °C.

and lithium ions are displaced by large alkylammonium ions. The pronounced broadening of the X-ray reflections indicates the structure to be highly disordered when the alkylammonium ions have penetrated between the layers. The *d*-value of the first broadened reflection at $2\theta \approx 9°$ indicates an average basal spacing of 1 nm which is independent of the alkyl chain length. This is expected when the alkyl chains lie parallel to the layers. The smallest spacing of this structure comprises the height of an alkyl chain (0.48 nm)[58] and that of the [SiO_4] tetrahedron (edge length O–O = 0.264 nm, $h = 0.264\sqrt{(2/3)} = 0.216$ nm)[9,13] increased by the van der Waals diameter of an oxygen atom (0.28 nm).[59] The sum $0.48 + 0.22 + 0.28 = 0.98$ nm agrees with the observed average basal spacing.

A further point must be considered when the alkyl chains lie flat between the layers. The unit cell ($a = 0.506$ nm, $b = 0.833$ nm, $c = 2 \times 0.719$ nm, $\beta = 96.6°$, $Z = 4$)[33] (Fig. 1) contains 8 cations. The area occupied by one cation (equivalent area) is $0.506 \times 0.833/4 = 0.10\ nm^2\ cation^{-1}$. An alkylammonium ion with 4 carbon atoms requires an area of $0.57 \times 4 + 1.4 = 0.368\ nm^2$.[58] Thus, only a part of the inorganic cations can be replaced by flat-lying alkylammonium ions. The remaining lithium and sodium ions are exchanged by protons because all inorganic cations were displaced. As a consequence a large number of silanol groups (Q^3 groups) are formed which promote disintegration of the structure when they condense to siloxane groups (Q^4 groups). Formation of Q^4 groups is clearly seen in the ^{29}Si-MAS-NMR spectra. The slight variation of the chemical shift of the Q^4 and also Q^3 groups (Table 3) with the chain length indicates that the structural rearrangements are chain length dependent. The smaller alkylammonium ions can adapt to the flexible tetrahedral layers more easily than longer chains. The decrease of the chemical shift of the Q^3 groups from δ −99.8 (methylammonium ions) to −100.5 (hexylammonium ions) is related to the changing environment of the silanol groups. The increase of the chemical shift at longer chain lengths indicates a different type of rearrangement. In addition, neoformation of a second phase with a sharp low-angle reflection is observed in the X-ray diagrams.

Formation of a large proportion of Q^4 groups also accompanies the transformation of silinaite into the crystalline silicic acid.[34] The corresponding ^{29}Si-MAS-NMR spectrum is very similar to the spectra of the alkylammonium derivatives. However, the pronounced disintegration of the structure which accompanies the alkylammonium ion exchange is not observed. The X-ray powder diagram of the crystalline acid shows relatively sharp reflections[34] in contrast to the largely broadened reflections of the alkylammonium derivatives. It is evident that the bulky alkylammonium ions render difficult an orderly condensation of silanol groups between adjacent layers,

Table 3 Mesopore and micropore volumes and diameters of the trimethylalkylammonium derivatives of silinaite

Sample	Total amount N_2 ads./$\mu L\ g^{-1}$[a]	Micropore volume/$\mu L\ g^{-1}$[b]	Mesopore volume/$\mu L\ g^{-1}$[c]	Diameter/nm[d]
DDTMA, 550 °C	154.7	25.7	129.0	1.9
TDTMA, 350 °C	289.3	75.2	214.1	2.6
TDTMA, 450 °C	317.2	59.6	257.6	2.3
TDTMA, 550 °C	191.9	50.2	141.7	1.7
HDTMA, 550 °C	498.2	109.7	388.5	2.9
HDTMA + TEA, 550 °C	170.2	30.9	139.2	2.8
CP, 550 °C	170.2	38.0	132.2	2.9

[a]From the isotherm at $p/p_0 \approx 0.5$. [b]From *t*-plot, see Table 2. [c]Total amount adsorbed minus micropore volume. [d]From eqn. (2).

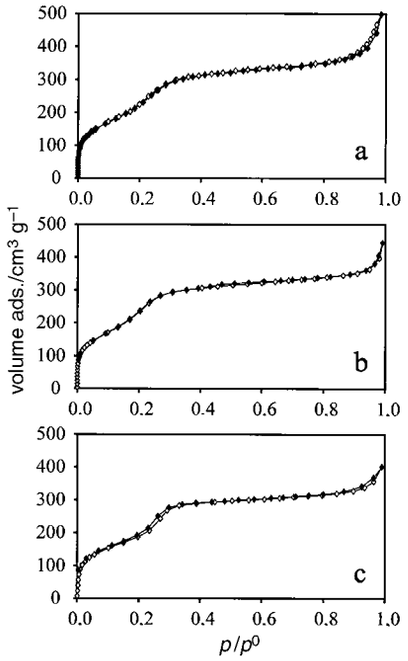

Fig. 10 N_2 adsorption isotherms (◇ adsorption, ◆ desorption, cm^3 N_2 (STP) g^{-1}, 77 K) of the HDTMA derivative (calcined at 550 °C) of a) silinaite, b) metasilicate, c) water glass solution.

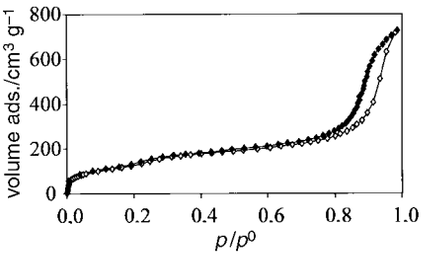

Fig. 11 N_2 adsorption isotherm (◇ adsorption, ◆ desorption, cm^3 N_2 (STP) g^{-1}, 77 K) of the TDTMA derivative of δ-$Na_2Si_2O_5$ (SKS-6) calcined at 550 °C.

instead condensation causes a pronounced disintegration of the structure.

Porous materials

Nitrogen adsorption of the calcined products (Figs. 7, 9, 10) gives isotherms like the calcined kanemite derivatives[6–9,11] and other mesoporous materials.[52,60–63] This type of isotherm is now called type IVc.[52] Characteristic is the absence of a hysteresis loop because of the pores being open at both ends and of the narrow pore size distribution. The amount of nitrogen adsorbed at the plateau corresponds to the mesopore volume v_p. The mean pore radius can be calculated from the mesopore volume and the specific surface area:

$$\bar{r}_p = 2v_p/S \quad (2)$$

S is the specific surface area confined to the cylindrical pore walls.[52,64] If micropores are also present, the value of the specific area has to be calculated from the *t*-plot. This diagram gives the micropore volume and the specific area of the outside of the particles. If mesopores are present (in addition to micropores) the area comprises the external area together with the area of the mesopore walls.[51] We assume that the contribution of the external area is small compared with the area of the mesopore walls. The value of S required in eqn. (2) then corresponds to the surface area calculated from the slope of the linear branch of the *t*-plots. The amount of gas adsorbed at the plateau consists of the micropore volume and the mesopore volume (Table 3). To calculate the average pore diameter using eqn. (2) we used the plateau value minus the micropore volume.

The pore diameters (Table 3) are in the range of values reported for other mesoporous materials.[6,8,52,62,64] The average pore diameter of the trimethylalkylammonium silinaites calcined at 550 °C decreases from the DDTMA derivative (d = 1.9 nm) to the TDTMA derivative (d = 1.7 nm, then increases to d = 3.0 nm (HDTMA). Higher calcination temperatures decrease the average diameter.

The *t*-plots of the calcined samples are typical of mesoporous materials which also contain micropores.[51] They are linear at low relative pressures and show an upward deviation at p/p_0 = 0.3–0.4. The linear section gives micropore volumes of 25–110 μL g^{-1} (Table 2). The micropore volumes of the HDTMA derivatives of δ-$Na_2Si_2O_5$, metasilicate and water glass are 56, 113, and 85 μL g^{-1} (Table 4).

The upward deviation of the *t*-curves commences at the relative pressure at which the mesopores are just being filled. The apparent diameter of these pores can be estimated from the Kelvin equation:[51]

$$r_c = 4.078/\log(p_0/p) \quad (3)$$

with r_c = core radius, $r_p = r_c + t$, r_p = pore radius and t = statistical thickness of the adsorbed film. The relative pressures at the beginning upward deviation are 0.29–0.32 and indicate core diameters of 1.5–1.7 nm. With $t \approx 0.5$ nm the apparent diameter of the pores is 2.5–2.7 nm and is comparable to the mesopore diameters calculated from eqn. (2) (Tables 3, 4).

Mechanism

In previously reported studies[4–11] kanemite was treated with trimethyl alkylammonium ions under somewhat severe conditions (primary alkylammonium ions are less suited because they are deprotonated at the initial high pH) and the formation of a new phase characterized by a sharp low-angle reflection was observed. However, such reflections are also observed when silinaite is simply reacted with primary alkylammonium ions at 65 °C for a few hours. Mesoporous materials obtained by templating rod-shaped micelles showed similar sharp low-angle reflections.[61,62,64,65] The reflection is considered as the (100) reflection of the hexagonal honeycomb structure. The lattice parameter (distance between the tubes) is then $a = 2d_{100}/\sqrt{3}$.[8,64]

Folding of the silicate layers around cylindric aggregates of alkylammonium ions was assumed.[4–11] Since different parent silicates (kanemite, silinaite, Na_2SiO_3, δ-$Na_2Si_2O_5$) and even

Table 4 Specific surface area, micropore, and mesopore volume of the HDTMA derivatives of silinaite, metasilicate, δ-$Na_2Si_2O_5$ and water glass solution

	Specific surface area/m^2 g^{-1} [a]	Total amount N_2 ads./μg $^{-1}$ [b]	Micropore volume/μL g^{-1} [a]	Mesopore volume/μL g^{-1} [c]	Diameter/nm [d]
Silinaite	529	498.2	109.7	388.5	2.9
Metasilicate	521	479.6	113	366.6	2.8
δ-$Na_2Si_2O_5$	346	309.4	55.6	253.8	2.9
Water glass	524	464.2	85	379.2	2.9

[a]From the linear *t*-plot at low p/p_0. [b]From the isotherm at $p/p_0 \approx 0.5$. [c]Total amount adsorbed minus micropore volume. [d]From eqn. (2).

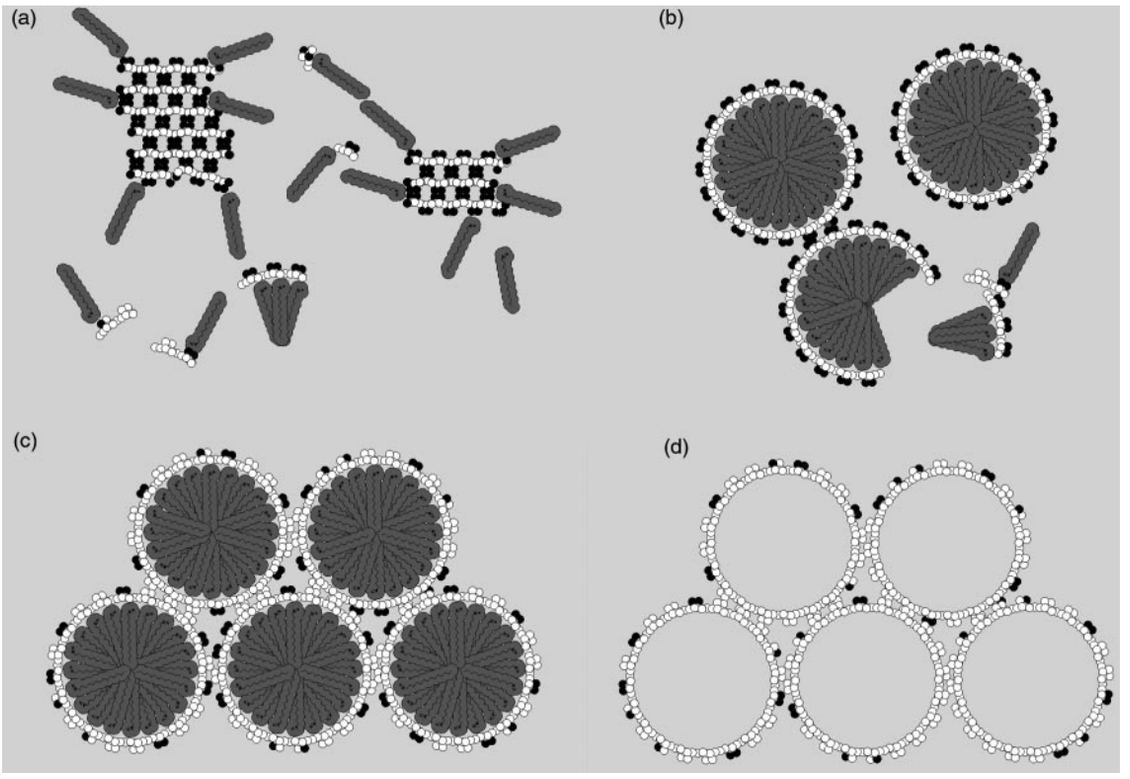

Fig. 12 Proposed mechanism of formation of the mesoporous material from silinaite and similar single-layer phyllosilicates (only oxygen atoms are shown: ○, between two Si, ●, of SiO^- or SiOH): (a) partial destruction of the silicate structure by alkylammonium ions which carry fragments of the silicate layers; (b), (c) aggregation of alkylammonium ions + fragments of the silicate layers; (d) formation of meso- and micropores during calcination.

water glass solutions yield nearly identical mesoporous materials, another mechanism is more likely. As discussed above, cation exchange with alkylammonium ions largely disintegrates the structure. The colloidal fragments and dissolved species then reaggregate under the influence of the alkylammonium ions (Fig. 12).

Formation of MCM-41 materials was originally proposed as a templating process in which dissolved silica species aggregate and condense around cylindrical micelles of surfactants. However, it was found that the surfactants can self-assemble into new ordered morphologies that are different from the initial micelle structure in the precursor surfactant solution. The inorganic phase can modify the organization of the organic array.[66–68]

In the case of the disintegrated alkylammonium silicates a direct templating process is unlikely because the alkylammonium ions are tightly attached to the silicate layers. After disintegration of the layers the alkylammonium ions carry the fragments of the layers and then aggregate to cylindrical forms. After calcination, the mesopore volume mainly comprises the pores of the hollow tubes. Micropores are formed between the tubes (*cf.* Fig. 12c,d). In a simple model the micropore volume is calculated from a hexagonal arrangement of tubes with a certain pore diameter, for instance 2.6 nm (TDTMA–silinaite calcined at 350 °C). Assuming a wall thickness of 0.9 nm,[9] one calculates a maximum mesopore volume of 458 $cm^3\ g^{-1}$ and a micropore volume of 86 $cm^3\ g^{-1}$. The observed volumes are of this order of magnitude (Table 3).

This model of micropore formation implies that the Si–OH or $Si–O^-$ bonds are directed to the ammonium ions whereas the more hydrophobic siloxane groups of the silicate layer fragments aggregate forming the walls of the micropores. Thereofore, the use of a standard isotherm for the *t*-plots calculated for smaller BET *C*-values is more appropriate than the usual standard isotherm for hydrophilic silica.

The aggregation of the alkylammonium ions with caps of fragmentated silicate layers may not be restricted to cylindrical arrays. The situation may be similar to the aggregation of surfactants which is directed by the size of the polar head groups and the hydrophobic tails.[69,70] The type of aggregate depends on the ratio v/al with v = volume of the tail, a = area of the head group, and l = full length of the tail. Spherical micelles form when $v/al < 0.33$ whereas cylindrical micelles occur at $0.33 < v/al < 0.5$ and vesicles or bimolecular layers at $0.5 < v/al < 1$. In a similar way the size ratio of the layer fragments and the alkyl chains may control the type of aggregation of alkylammonium ions carrying fragments of the silicate layer. The importance of geometric conditions and electrostatic factors was stressed by Fu *et al.*[71] These authors presented a nice example of formation of a lamellar phase when the electrostatic repulsion between the head groups was reduced by the incorporation of deprotonated alkylammonium ions.

Other types of organic arrays could be prepared from single layer phyllosilicates and transformed into porous materials when the appropriate conditions for alkylammonium exchange and calcination procedure are identified. The very structure of the pore walls should be dependent on the type of the silicate layer fragments the alkylammonium ions carry with them. Probably, differences are more evident from the thermal behavior than from the pore volumes. Inagaki *et al.*[4,8] reported that the mesoporous materials formed after heating the alkylammonium kanemite at between 550 °C and 900 °C whereas the silinaite derivatives transformed into quartz at $\geqslant$ 700 °C.

Acknowledgements

We acknowlege the assistence of Dr. G. Peters, Institute of Inorganic Chemistry, University of Kiel, during the MAS measurements and thank him for his cooperation. We are

grateful to the Fonds der Chemischen Industrie for financial support.

References

1 *Appl. Clay Sci.*1999, **15**(1),
2 Z. Wang, T. Lau and T. J. Pinnanvaia, *Chem. Mater.*, 1996, **8**, 2200.
3 Z. Wang and T. J. Pinnavaia, *Chem. Mater.*, 1998, **10**, 1820.
4 S. Inagaki, Y. Fukushima and K. Kuroda, *J. Chem. Soc., Chem. Commun.*, 1993, 680.
5 S. Inagaki, Y. Fukushima, A. Okada, T. Kurauchi, K. Kuroda and C. Kato, *Proc. 9th Int. Zeolite Conf., Montreal, 1992*, ed. R. von Ballmoos *et al.*, Butterworth-Heinemann, Boston, MA, 1993, p. 305.
6 P. J. Branton, K. Kaneko, N. Setoyama, K. S. W. Sing, S. Inagaki and Y. Fukushima, *Langmuir*, 1996, **12**, 599.
7 T. Kimura, S. Saeki, Y. Sugahara and K. Kuroda, *Langmuir*, 1999, **15**, 2794.
8 S. Inagaki, A. Koiwai, N. Suzuki, Y. Fukushima and K. Kuroda, *Bull. Chem. Soc. Jpn.*, 1996, **69**, 1449.
9 S. Inagaki, Y. Sakamoto, Y. Fukushima and O. Terasaki, *Chem. Mater.*, 1996, **8**, 2089.
10 Y. Kitayama, H. Asano, T. Kodama, J. Abe and Y. Tsuchiya, *J. Porous Mater.*, 1998, **5**, 139.
11 H. Hata, S. Saeki, T. Kimura, Y. Sugahara and K. Kuroda, *Chem. Mater.*, 1999, **11**, 1110.
12 H. Miyata and K. Kuroda, *Adv. Mater.*, 1999, **11**, 857.
13 F. Liebau, *Structural Chemistry of Silicates*, Springer-Verlag, Berlin, 1985.
14 G. Lagaly, *Silicates*, in *Ullmann's Encyclopedia of Industrial Chemistry*, Wiley-VCH, Weinheim, 1993, vol. A23, p. 661.
15 F.-J. Dany, W. Gohla, J. Kandler, H.-P. Rieck and G. Schimmel, *Seifen-Öle-Fette-Wachse*, 1990, **116**, 805.
16 D. Heidemann, C. Hübert, W. Schwieger, P. Grabner, K.-H. Bergk and P. Sarv, *Z. Anorg. Allg. Chem.*, 1992, **617**, 169.
17 V. Kahlenberg, G. Dörsam, M. Wendschuh-Josties and R. X. Fischer, *J. Solid State Chem.*, 1999, **146**, 380.
18 K. Beneke and G. Lagaly, *Am. Mineral.*, 1977, **62**, 763.
19 W. Schwieger, W. Heyer, F. Wolf and K.-H. Bergk, *Z. Anorg. Allg. Chem.*, 1987, **548**, 204.
20 K.-H. Bergk, W. Schwieger and M. Porsch, *Chem. Technol.*, 1987, **39**, 459; K.-H. Bergk, W. Schwieger and M. Porsch, *Chem. Technol.*, 1987, **39**, 508.
21 I. A. Crone, K. R. Franklin and P. Graham, *J. Mater. Chem.*, 1995, **5**, 2007.
22 W. Wieker, D. Heidemann, R. Ebert and A. Tapper, *Z. Anorg. Allg. Chem.*, 1995, **621**, 1779.
23 D. C. Apperley, M. J. Hudson, M. T. J. Keene and J. A. Knowles, *J. Mater. Chem.*, 1995, **5**, 577.
24 G. G. Almond, R. K. Harris, K. R. Franklin and P. Graham, *J. Mater. Chem.*, 1996, **6**, 843.
25 G. G. Almond, R. K. Harris and K. R. Franklin, *J. Mater. Chem.*, 1997, **7**, 681.
26 S. Hayashi, *J. Mater. Chem.*, 1997, **7**, 1043.
27 Y. Huang, Z. Jiang and W. Schwieger, *Microporous Mesoporous Mater.*, 1998, **26**, 215.
28 S. Vortmann, J. Rius, B. Marler and H. Gies, *Eur. J. Mineral.*, 1999, **11**, 125.
29 R. Wey and A. Kalt, *C. R. Acad. Sci. Paris*, 1967, **265**(1), 101.
30 M.-T. Le Bihan, A. Kalt and R. Wey, *Bull. Soc. Fr. Minéral. Cristallogr.*, 1971, **94**, 15.
31 D. Benbertal and A. Mosset, *J. Solid State Chem.*, 1994, **108**, 340.
32 G. Y. Chao, J. D. Grice and R. A. Gault, *Can. Mineral.*, 1991, **20**, 359.
33 J. D. Grice, *Can. Mineral.*, 1991, **29**, 363.
34 K. Beneke, P. Thiesen and G. Lagaly, *Inorg. Chem.*, 1995, **34**, 900.
35 H. Annehed, L. Fälth and F. J. Lincoln, *Z. Kristallogr.*, 1982, **159**, 203.
36 W. Schwieger, K. H. Bergk, D. Heidemann, G. Lagaly and K. Beneke, *Z. Kristallogr.*, 1991, **197**, 1.
37 M. Hanaya and R. K. Harris, *Solid State Nucl. Magn. Reson.*, 1997, **8**, 147.
38 W. Schwieger, D. Heidemann and K.-H. Bergk, *Rev. Chim. Mineral.*, 1985, **22**, 639.
39 D. Heidemann, W. Schwieger and K.-H. Bergk, *Z. Anorg. Allg. Chem.*, 1987, **555**, 129.
40 R. K. Iler, *J. Colloid Polym. Sci.*, 1964, **19**, 648.
41 G. Lagaly, K. Beneke and A. Weiss, *Am. Mineral.*, 1975, **60**, 642.
42 R. A. Fletcher and D. M. Bibby, *Clays Clay Miner.*, 1987, **35**, 318.
43 W. Schwieger, W. Heyer and K.-H. Bergk, *Z. Anorg. Allg. Chem.*, 1988, **559**, 191; W. Schwieger, W. Heyer and K.-H. Bergk, *Z. Anorg. Allg. Chem.*, 1992, **600**, 139.
44 K. Beneke and G. Lagaly, *Am. Mineral.*, 1989, **74**, 224.
45 A. Brandt, W. Schwieger, K.-H. Bergk, P. Grabner and M. Porsch, *Cryst. Res. Technol.*, 1989, **24**, 47.
46 M.-J. Binette and C. Detellier, *Clays Clay Miner.*, 1998, **46**, 478.
47 G. Scholzen, K. Beneke and G. Lagaly, *Z. Anorg. Allg. Chem.*, 1991, **597**, 183.
48 K. Beneke and G. Lagaly, *Am. Mineral.*, 1983, **68**, 818.
49 H.-H. Kruse and G. Lagaly, *GIT-Fachz. Lab.*, 1988, **32**, 1096.
50 H.-H. Kruse, K. Beneke and G. Lagaly, *Colloid Polym. Sci.*, 1989, **267**, 844.
51 S. J. Gregg and K. S. W. Sing, *Adsorption, surface area and porosity*, Academic Press, London, 2nd edn., 1982, pp. 77, 96, 135, 214.
52 F. Rouquerol, J. Rouquerol and K. Sing, *Adsorption by powders & porous solids*, Academic Press, San Diego, 1999, pp. 199, 415ff, 440.
53 A. L. McCleelan and H. F. Harnberger, *J. Colloid Polym. Sci.*, 1967, **23**, 577.
54 A. Lecloux and J. P. Pirard, *J. Colloid Interface Sci.*, 1979, **70**, 265.
55 Y. Huang, Z. Jiang and W. Schwieger, *Chem. Mater.*, 1999, **11**, 1210.
56 Y. Huang, Z. Jiang and W. Schwieger, *Can. J. Chem.*, 1999, **77**, 495.
57 E. P. Barrett, L. G. Joyner and P. P. Halenda, *J. Am. Chem. Soc.*, 1951, **73**, 373.
58 W. B. Innes, *Chem. Ind.*, 1957, 757.
59 H. Fabre and G. Lagaly, *Clay Miner.*, 1991, **26**, 19.
60 G. Lagaly and A. Weiss, *Kolloid Z. Z. Polym.*, 1971, **243**, 48.
61 T. Endo, M. M. Mortland and T. J. Pinnavaia, *Clays Clay Miner.*, 1980, **28**, 105.
62 P. J. Branton, P. G. Hall, K. S. W. Sing, H. Reichert, F. Schüth and K. K. Unger, *J. Chem. Soc., Faraday Trans.*, 1994, **90**, 2965.
63 C. T. Kresge, M. E. Leonowicz, W. J. Roth, J. C. Vartuli and J. S. Beck, *Nature*, 1992, **359**, 710.
64 J. Kim and R. Ryoo, *Chem. Mater.*, 1999, **11**, 487.
65 K. J. Edler and J. W. White, *J. Chem. Soc., Chem. Commun.*, 1995, 155.
66 R. Schmidt, E. W. Hansen, M. Stöcker, D. Akporiaye and O. H. Ellestad, *J. Am. Chem. Soc.*, 1995, **117**, 4049.
67 C. A. Fyfe and G. Fu, *J. Am. Chem. Soc.*, 1995, **117**, 9709.
68 V. Alfredson, M. Keung, A. Monnier, G. D. Stucky, K. Unger and F. Schüth, *J. Chem. Soc., Chem. Commun.*, 1994, 921.
69 Q. Huo, D. L. Margolese, U. Ciesla, P. Feng, T. E. Gler, P. Sieger, R. Leon, P. M. Petroff, F. Schüth and G. D. Stucky, *Nature*, 1994, **368**, 317.
70 A. Firouzi, D. Kumar, L. M. Bull, T. Besier, P. Sieger, Q. Huo, S. A. Walker, J. A. Zasadzinski, C. Glinka, J. Nicol, D. Margolese, G. D. Stucky and B. F. Chmelka, *Science*, 1995, **267**, 1138.
71 J. N. Israelachvili, D. J. Mitchell and B. W. Ninham, *J. Chem. Soc., Faraday Trans. 2*, 1976, **72**, 1525.
72 H. Hoffmann and G. Ebert, *Angew. Chem.*, 1988, **100**, 933.
73 G. Fu, C. A. Fyfe, W. Schwieger and G. T. Kokotailo, *Angew. Chem.*, 1995, **107**, 1582.